

# Shortcut Removal for Improved OOD-Generalization

Nicolas M. Müller \*  
 Fraunhofer AISEC, Germany  
 nicolas.mueller@aisec.fraunhofer.de

Jennifer Williams  
 University of Southampton, UK  
 J.Williams@soton.ac.uk

Jochen Jacobs \*  
 TU Munich, Germany  
 jochen.jacobs@tum.de

Konstantin Böttinger  
 Fraunhofer AISEC, Germany  
 konstantin.boettinger@aisec.fraunhofer.de

## Abstract

Machine learning is a data-driven discipline, and learning success is largely dependent on the quality of the underlying data sets. However, it is becoming increasingly clear that even high performance on held-out test data does not necessarily mean that a model generalizes or learns anything meaningful at all. One reason for this is the presence of machine learning shortcuts, i.e., hints in the data that are predictive but accidental and semantically unconnected to the problem. We present a new approach to detect such shortcuts and a technique to automatically remove them from datasets. Using an **adversarially trained lens**, any small and highly predictive clues in images can be detected and removed. We show that this approach 1) does not cause degradation of model performance in the absence of these shortcuts, and 2) reliably identifies and neutralizes shortcuts from different image datasets. In our experiments, we are able to recover up to 93,8% of model performance in the presence of different shortcuts. Finally, we apply our model to a real-world dataset from the medical domain consisting of chest x-rays and identify and remove several types of shortcuts that are known to hinder real-world applicability. Thus, we hope that our proposed approach fosters real-world applicability of machine learning.

## 1 Introduction

Shortcuts in machine-learning data are a type of false-feature that strongly correlates with the target class. They are easy to learn by a neural network, but are not expected to be present when applying the network

in the real world. These shortcuts may originate from the data collection process or technique, or from the type of data being collected. For example, when training on a binary-class image dataset where all images of class 0 have watermarks and all images of class 1 do not, the neural network can rely on the presence of the watermark to predict the class. A famous real-world example is the Pascal VOC 2007 dataset [1], where all images of horses contained the photographer’s watermark in the lower-left corner [12]. Difficult cases of shortcuts may also exist and it is not always possible to identify shortcuts during data collection or pre-processing steps. When naively training a learning model on such data that contains shortcuts, the high predictive power of the shortcut can coax a model to rely heavily on irrelevant features that cannot generalize. This incurs seemingly high performance even on held-out data, provided the shortcut is present, which may be true if the held-out data is sampled via the same process. It will seem as though the model has learned its task, although it uses only the shortcut, and has not learned the desired semantics of the task. Therefore the network will not be able to work properly when applied to real-world data – generally referred to as out-of-distribution (OOD) data. Generalization to OOD data – or *Domain Generalization* – is a very prominent problem in machine learning [26].

In this paper we make the following contributions:

- Present a new architecture that allows neural networks to learn the real features of a dataset during training, where the data contains known or unknown shortcuts.
- Use an adversarially trained *neural lens* to remove all simple shortcut features that the network mistakenly pays attention to. At the same time, the lens also provides a visual representation of the shortcuts that are avoided.

---

\*equal contribution

We show that our model 1) reliably identifies different shortcuts in several datasets, 2) successfully inpaints the training data to neutralize the shortcut, and 3) does not deteriorate the model if no shortcuts are present. We apply our model to a real-world dataset of chest x-rays (raw chest x-ray images from the COVID QU-Ex[21] dataset), identifying and neutralizing several shortcuts in this real-world dataset.

## 2 Related Work

### 2.1 Machine Learning Shortcuts

Shortcuts in training data come in a large variety. A prominent case are logos and other local marks in image datasets. For example, the Pascal VOC 2007 dataset [1] contains a watermark on horse photos [12]. This problem is also common in chest x-ray images where hospital- or device-specific marks are common [25, 5].

Shortcuts can, however, also be of a more global nature. For example, a pasture can be an easy clue for the class “Cow” [3]. Work from [7] provides an overview of many different global shortcuts. Dealing with these global shortcuts is part of the wider research area of *Domain Generalization* [26]. In this paper, we will focus on local shortcuts instead, as these in particular prevent the use of machine learning on important real-world problems [5].

The presence of shortcuts is an especially significant problem in self-supervised representation learning, which relies on a feature extractor to learn a wide range of features [8]. The presence of shortcuts with regard to the pretext task thus significantly limits the usability of the pre-trained feature extractor [6, 14] – especially since these shortcuts are not predictive of the later “real” task. From this flows our motivation to render shortcuts harmless directly during the training process.

Shortcuts are not limited to image datasets. For example, in the ASVspoof Challenge Dataset on audio deepfake detection [22], the amount of leading silence can be used to predict the target class [15]. We believe our proposed technique can benefit the wider machine learning community, as this is a prominent problem for all machine learning tasks.

### 2.2 Automatic shortcut removal

Automatic shortcut removal has been proposed [14] for self-supervised representation learning. This was done by adding U-Net [18] in front of the classification network. The authors coined the term “lens” for their

U-Net, thus we have adopted the term in our work. The lens is trained adversarially on the negative loss of the classification network and an additional reproduction loss. Here, [14] used a pixel-wise  $L_2$  loss. A hyper-parameter  $\lambda$  is introduced to control the weight of the reproduction loss. The capacity of the lens network is chosen deliberately small such that the lens can only remove simple features (i.e. shortcuts). However, [14] is only suitable for self-supervised learning. To the best of our knowledge, we are the first to present an appropriate architecture for classification.

Finally, in order to prevent a network from paying too much attention to shortcuts that are only present in a subset of the dataset, [4] proposes to use weighted training: Images that can be classified well by a low-capacity network are assumed to contain shortcuts and are therefore weighted lower when training the high-capacity network. However, this method fails to work if a large majority of images contain shortcuts. Since our approach detects shortcuts via an adversarial component, there is no need to weight the training data according to low- or high-capacity network performance. Thus, our approach is not limited by an upper bound on the number of shortcut-affected data. In fact, we show that our approach also works with 100% shortcuts per class, c.f. Sec. 4.2.

### 2.3 Adversarial autoencoders

Adversarial autoencoders have been proposed by [2] and [16]. They add an autoencoder in front of a classification network and train the autoencoder adversarially to produce images that look similar to the original input, but then trick the classifier to output a wrong class. Work from [16] additionally proposes to use an autoencoder to produce image-agnostic perturbations. Further, [23] proposes AdvGAN by adding a GAN-Discriminator as an additional loss for the autoencoder. This leads to less perceptible perturbations. While these methods use very similar architectures to the one we propose here, none use the generated adversarial images to robustly train the classifier. In fact, our method combines adversarial training and adversarial autoencoders.

## 3 Architecture

To remove shortcuts in supervised problems, we adopt a lens network, first described in [14], to the supervised domain. A low-capacity Image-to-Image network (called ‘Lens Network’) is placed in front of the classification network. This lens is then trained jointly, but

Figure 1: Architecture of our proposed *attention lens* model. The lens (red) consists of an Attention module  $A$  and a Reconstruction module  $R$ , both of which are U-Nets. The output of the Lens is passed to the original classifier (blue), trained via cross-entropy loss. Optionally, input images are also passed to the original classifier. The lens is trained via the classifier’s inverted gradients (via the gradient-reversal layer) and a reproduction penalty loss  $L_{repr}$ .

adversarially, with the classifier to decrease its performance. The idea is that the lens is trained to isolate features of the image that the classification network is paying attention to. Since the capacity of the lens is limited, only simple features (i.e. shortcuts) can be removed by the lens. To further enforce this, we extend the training loss with an additional reproduction loss  $L_{repr}$ . This ensures that the lens modifies the original image only slightly.

We investigate two different lens architectures. Firstly, a *simple lens* consisting of a simple U-Net. This resembles the architecture used by [14]. As stated, the size and receptive field of this U-Net should be limited such that it can only modify simple features. Secondly, inspired by [17], we propose a more advanced lens architecture, which we term *attention lens*. Our proposed solution uses two networks, an attention network  $A$  and a replacement network  $R$ . Network  $A$  decides *where* in the original image the shortcut is located, while network  $R$  computes *what* a suitable replacement should be. An overview of our proposed architecture using the attention lens is illustrated in Fig. 1.

Both the attention and replacement networks are U-Nets that receive the original image  $I \in D^{c,w,h}$  as input, where  $D$  is the transformed range of the image,  $c$  is the channel dimension, and  $w, h$  are the image’s width and height, respectively. The attention network  $A$  has a single channel output with sigmoid activation to ensure an output in  $[0, 1]^{w,h}$ . The replacement network  $R$  outputs a tensor in  $\mathbb{R}^{c,w,h}$  which is clipped to  $D^{c,w,h}$ . This full lens network then outputs an inpainted image, which is derived via

$$A \cdot R + (1 - A) \cdot I \quad (1)$$

The size of the attention network affects the complexity of the shortcuts that can be identified, and should thus be chosen appropriately for the problem domain. The task of the replacement network is more complex than that of the attention network, therefore we accord a larger model capacity to  $R$  than to  $A$ .

The U-Nets used for the simple lens as well as the attention and replacement modules of the attention lens are constructed from a number of downsampling steps. Each step consists of a sequence of a 3x3 convolution, 2x2 max-pooling, followed by two times up-sample and

3x3 convolution. The innermost layer consists of two 3x3 convolutions. We use batch normalization [10] and LeakyReLU [24] after each layer. We can control the capacity of the networks by changing the number of downsampling steps.

### 3.1 Training Loss

As stated previously, we train the lens and classifier jointly using a single loss:

$$L = \lambda L_{repr} + L_{CE} \quad (2)$$

where  $L_{CE}$  is the cross entropy loss of the classification network  $C$  and  $\lambda$  is a hyperparameter controlling how much the lens is allowed to modify the input image. Note that the cross-entropy loss trains both the classifier, as well as the lens network adversarially via a gradient reversal layer.  $L_{repr}$  does not influence the classifier, c.f. Fig. 1. The choice of the reproduction loss  $L_{repr}$  depends on the lens architecture. For the simple lens, we use an  $L_2$  loss between the input image and the lens output, as was used by [14].

For the attention lens we only restrict the attention module using an attention loss while the reconstruction module remains unrestricted:

$$L_{repr} = \max \left( \rho, \frac{1}{wh} \sum_{ij} A_{ij} \right) - \rho. \quad (3)$$

Here,  $\rho \in [0, 100\%]$  is the hinge hyperparameter that controls the percentage of the image that can be modified without penalty.

### 3.2 Model Oscillation

We observe that there can be oscillation during training. Once the shortcuts in the data are removed, the classifier will no longer pay attention to them, causing the lens to no longer remove them. We can partially counteract this by passing some images directly to the classifier, omitting the lens network. In our experiments, we pass each image to the classifier twice: once passing through the lens network and once bypassing it. This makes the classifier focus on the shortcuts

more consistently, which attenuates oscillation of the lens network during training.

## 4 Datasets

This section presents the datasets we use to evaluate our proposed model. We present two evaluation approaches. We evaluate our proposed model on a set of artificially introduced shortcuts on CIFAR10 and ImageNet. This allows fine-grained analysis since we control the presence of the shortcuts. Additionally, we apply our model to a real-world dataset (covid-qu-Ex [21]) and present an analysis of the shortcuts that the model identified.

### 4.1 CIFAR10

We use one of the most popular computer vision datasets, the CIFAR10 dataset [11], to which we add a number of different shortcuts:

- Color Dot, where we add a circle at a random position in the image. The color of the dot corresponds to the target class labels.
- Location Dot, where we add a circle of random color at coordinates  $(x, y)$ . While  $x$  is chosen randomly, the vertical component  $y$  perfectly correlates with the target class.
- Hue Adaptation, where the hue of the image indicates the target class.

### 4.2 ImageNet

Additionally, we evaluate the lens on the ImageNet dataset [19], which features higher-resolution images than CIFAR. Here, we experiment with a two-class setup, where the two classes are visually similar, in our case “goose” and “pelican”. This corresponds to many real-world problems where the images between classes are visually similar, for example with analysis of medical images. To make the images even more similar, we convert them to grayscale.

We add shortcuts by adding an overlay. We use one of two different overlays:

- Logo: we add a single logo to a random position of the image
- Watermark: we add a “Stock Photo” text watermark across the entire image.

Each of the above-mentioned overlays are added to the images in two different ways. First, the overlay is

added to all images of class “pelican”. Thus, the presence or absence of the overlay indicates the target class. Second, the (same) overlay is added to 98% of images of class “pelican” and 2% of images of class “goose”. This slightly limits the productiveness of the shortcut. Thus, in total, we explore four different configurations of machine-learning shortcuts on ImageNet.

### 4.3 covid-qu-Ex

Additionally, we evaluate the effectiveness on a real-world dataset by applying our model to the covid-qu-Ex [21]. It features x-ray images of the human chest. It contains 3 classes: healthy, COVID-19 and Non-COVID pneumonia. Chest x-ray images have been previously shown to contain shortcuts [25], especially when the images come from multiple sources (i.e. different hospitals). As mentioned previously, shortcuts in x-ray data have been shown to significantly hinder real-world application of machine learning [5].

The covid-qu-Ex dataset was collected from a number of different sources, with normal and non-COVID pneumonia images being significantly older than COVID images. A visual inspection of the dataset especially shows a large amount of text in the corners of the images that would be easy to detect if they are correlated to the target class.

We note that significant effort by [21] went into creating segmentation masks for both the lung area and the infection area, thus turning the classification task into a segmentation task. Their main motivation for using segmentation was to avoid the shortcuts contained in the data. Here, we will not use segmentation masks, but instead evaluate how the shortcuts affect the classification problem and how well our model can detect and neutralize them.

## 5 Experiments and Results

In this section, we present our experiments and findings with the curated datasets: CIFAR10 and ImageNet. We then present our experiments and findings on the real-world covid-qu-Ex dataset.

### 5.1 CIFAR10 and ImageNet Experiments

In our experiments, we use the ResNet18 [9] architecture. We train the network on CIFAR10 and ImageNet datasets with the shortcuts described in Sec. 4 as well as without shortcuts. We evaluate the training with no lens, the simple lens, and the attention lens as described in Sec. 3.

	Shortcut		No Lens	Simple Lens	Attention Lens
CIFAR10	None		<b>75.1 ± 2.4</b>	70.2 ± 2.3	<b>76.7 ± 2.3</b>
	Color Dot	$p = 100$	28.5 ± 0.9	54.1 ± 8.5	<b>70.5 ± 2.1</b>
	Location Dot	$p = 100$	41.9 ± 7.0	55.4 ± 4.5	<b>69.0 ± 3.2</b>
	Hue	$p = 100$	30.1 ± 1.0	<b>49.6 ± 6.2</b>	42.0 ± 5.4
ImageNet	None		<b>78.9 ± 1.1</b>	<b>76.8 ± 3.4</b>	<b>76.1 ± 2.8</b>
	Logo	$p = 100/0$	51.9 ± 2.0	65.5 ± 12.7	<b>74.1 ± 9.0</b>
	Logo	$p = 98/2$	53.8 ± 3.8	66.1 ± 15.4	<b>75.0 ± 6.1</b>
	Watermark	$p = 100/0$	52.4 ± 1.4	<b>60.9 ± 4.1</b>	<b>61.0 ± 5.2</b>
	Watermark	$p = 98/2$	53.5 ± 3.5	<b>58.1 ± 3.5</b>	<b>59.8 ± 3.4</b>

Table 1: The effect of the lens network, measured in test accuracy. For two datasets (CIFAR10 and ImageNet), we train a ResNet18 architecture on data that is either free of shortcuts (row 'None') or has shortcuts in the training data (rows Color Dot, Location Dot, Hue). We then evaluate how such a model performs on *clean* validation data. We train each architecture 3 times and report the mean test accuracy and 95% confidence interval.

For the simple lens approach, we use 5 downsampling steps and set  $\lambda = 5$ . Finding an appropriate value for  $\lambda$  proved difficult as it controls the amount of shortcuts that can be found as well as the amount any shortcut can be removed. This issue contributed to our decision to propose the more complex attention-based lens.

For our attention lens approach, we use  $\lambda = 15$ . The attention network  $A$  has 3 downsampling steps and the replacement network  $R$  has 5 downsampling steps. For the CIFAR-based experiments, we use  $\rho = 2.5\%$ , a classifier learning rate of  $3 \cdot 10^{-5}$ , classifier weight decay of  $1 \cdot 10^{-4}$  and a lens learning rate of  $1 \cdot 10^{-4}$ . For the ImageNet experiments, we use  $\rho = 5.0\%$  (logo shortcut) or  $\rho = 10.0\%$  (watermark shortcut), a classifier learning rate of  $1.5 \cdot 10^{-6}$ , classifier weight decay of 0.01, and lens learning rate of  $1 \cdot 10^{-4}$ . We chose a larger  $\rho$  for the watermark shortcut because it constitutes a significant part of the image.

We train the network for a total of 30 epochs on the CIFAR10 data, and 50 epochs on the ImageNet data. We run each experiment 3 times, evaluate the accuracy on a *clean* validation set without any shortcuts, and report the mean accuracy and 95% confidence interval in Tab. 1. From Tab. 1, we find the following. For the case of **lens and no shortcuts**, using the simple or attention lens, the validation accuracy does not deteriorate when training on data without shortcuts. For the case of **no lens and shortcuts**, once we include a learning shortcut into the dataset, the validation accuracy decreases significantly, while train accuracy is excellent. This indicates that the network has failed to learn the important features from the dataset and has only focused on the shortcuts. For the case of **lens and shortcuts**, both the simple and attention lens can mitigate the effects of the shortcuts on the training process. The attention lens performs best in removing

shortcuts that are localized to small areas of the image (i.e. the color dot, location dot, and logo shortcuts). Here, the negative impact of the shortcuts is almost completely remedied. Shortcuts that involve the entire image (i.e. the hue shortcut) are harder to remove. The attention lens does not provide any benefit over the simple lens in these cases.

Example outputs of the attention lens when training on the CIFAR10 color dot and location dot shortcuts are shown in Fig. 2. Those when training on the ImageNet watermark shortcut are shown in Fig. 3. We observe the following:

1. The attention lens is able to remove the shortcuts visually from the image.
2. The color dot shortcut is eliminated by recoloring the dots. This is sufficient as only the color of the dot is deterministic of the class.
3. The location dot shortcut can't be removed by recoloring the dots and thus the lens instead fills the dots with the predicted background.
4. The lens is partially removing the watermark shortcut by adding the watermark to the remaining images.

To determine the optimal  $\rho$  we repeated the CIFAR10 Location Dot experiment with varying values of  $\rho$ . We evaluate each of the different candidate values for  $\rho$  over three independent runs, and report the mean accuracy and 95% confidence interval in Fig. 4. We find that the optimal  $\rho$  with this shortcut is around  $\rho = 2.5\%$ . This roughly corresponds to the percentage of the image that the shortcut occupies. A much higher  $\rho$  results in the lens manipulating too much of the image resulting in poor performance of the classifier on original images.

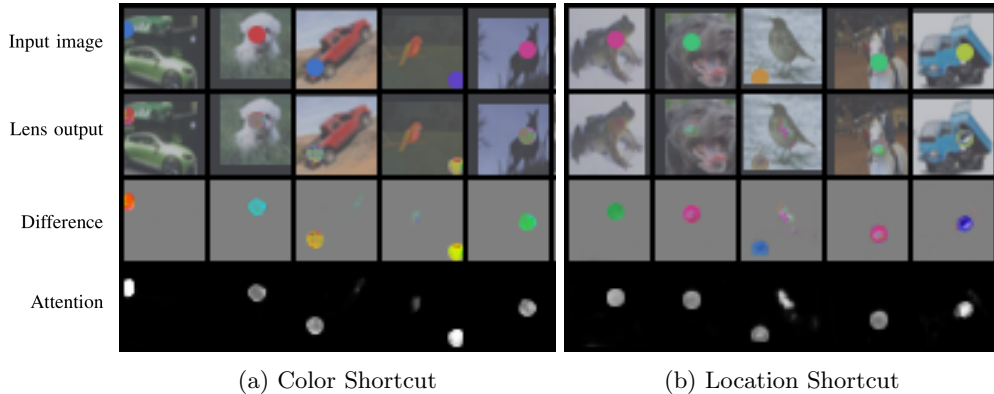


Figure 2: Examples of shortcuts and lens output on CIFAR10 training data. **Row 1** shows the input image with shortcut dots added: the target class is encoded in (a) the color of the dot or (b) the horizontal position of the dot. **Row 2** shows the output of the lens. **Row 3** shows the difference between rows 1 and 2. **Row 4** shows the output of the attention network  $A$ .

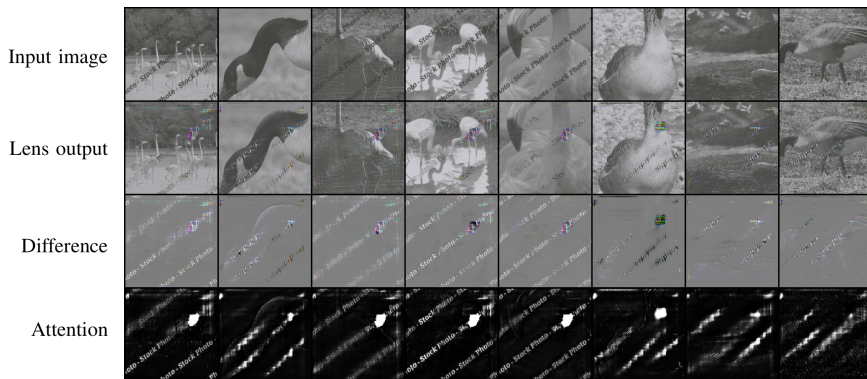


Figure 3: Examples of shortcuts and attention lens output on binary ImageNet training data. Images are of 2 classes (Pelican and Goose). **Row 1** shows the input image with the watermark shortcut added to 98% of all Pelican and 2% of all Goose images. **Row 2** shows the output of the lens. **Row 3** shows the difference between rows 1 and 2. **Row 4** shows the output of the attention network  $A$ .

## 5.2 covid-qu-Ex Experiments

For the covid-qu-Ex dataset, we train the network without a lens and with the attention lens with  $\lambda = 5$ ,  $\rho = 0.25\%$ , 2 downsample steps in the attention network and 5 downsample steps in the replacement network. We used a learning rate of  $2 \cdot 10^{-4}$  for both lens and classifier. As we do not have a validation set without shortcuts for covid-qu-Ex, we evaluate the effectiveness of the lens using GradCAM [20]<sup>1</sup>. Figure 5 shows the GradCAM images for all 3 classes and both trained networks. From these experiments, we make several observations. First, without the lens the network predominantly focuses on areas in the corners of

<sup>1</sup>As the class-discriminate CAM images are not desired in our case we use the absolute gradients rather than only positive gradients.

the images, mostly in areas with text. Second, with the attention lens, the network focuses on more relevant sections of the image, including the lung.

Figure 6 shows an example output of the lens during the training. We observe that the attention network mostly highlights text and other markers outside the lung area. This indicates that indeed these markers are the most prominent shortcut in the dataset. The lens is also able to remove most shortcuts from the images. Therefore, we can conclude that the attention lens is able to neutralize the text marker shortcuts that exist in the covid-qu-Ex x-ray images.

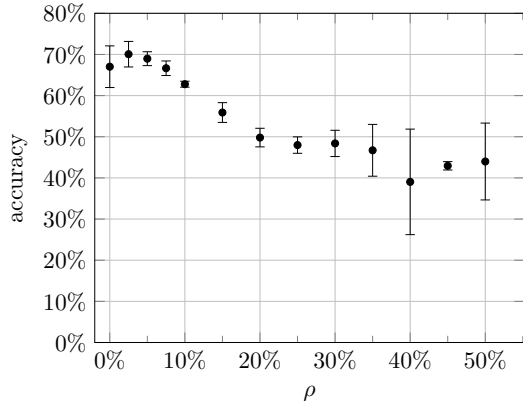


Figure 4: Accuracy on the *clean* validation set when training a classifier with the attention lens with varying  $\rho$  on the CIFAR10 dataset with the Location Dot shortcut. Experiment repeated three times for each value of  $\rho$ .

## 6 Discussion

As shown, the method we presented here is able to avoid shortcuts that exist in training data. As a result, the trained network will pay attention to “real” and semantically meaningful features. This particularly presents a solution if manual removal of shortcuts (i.e., in the form of segmentation masks) in the training data is prohibitively expensive or difficult. If, however, manual removal of shortcuts is possible (like in the covid-qu-Ex dataset), the achievable results will be superior to those achievable by our method.

The main limitation of our method is a result of the oscillation issues described in Sec. 3. The lens can only remove features that the classifier is paying attention to, while simultaneously trying to work around the fact that the classifier must attend to exactly meaningless features at some point during training, in order for them to be removed. As described in Sec. 3.2 this issue can be partially mitigated by additionally training the classification network on the original training data.

However, it remains impossible to prevent the classification network from occasionally paying attention to the shortcuts. While this method does archive the original goal of encouraging the network to *not only* pay attention to the shortcuts it must be emphasized that a limitation of our technique involves handling of contradictory shortcuts that can exist in the deployment environment. This method especially does not present a defense against backdoor adversarial attacks for image classification.

Furthermore, this architecture introduces new hyperparameters (size of the lens networks,  $\lambda$ , and  $\rho$ ).

It is difficult to find appropriate values for these hyperparameters in the absence of a validation set without shortcuts. Also, the required training of the lens networks is computationally expensive, resulting in a slowdown of the training process.

### 6.1 Potential Negative Societal Impacts

Our proposed approach increases the applicability and reliability of ML algorithms in the real world. This obviously has many positive effects (e.g. in medical scenarios), but, depending on the area of application, can also have negative consequences if, for example, fairness [13] and data protection are not sufficiently considered. In principle, however, the proposed approach is morally neutral and its ethical evaluation depends solely on the purpose of use and thus on the person using it.

### 6.2 Future Work

The model we presented in this paper can mostly only handle local shortcuts. This results from the restrictive reproduction loss we impose on the lens. While some reproduction loss is necessary to ensure the lens is not just returning random noise, a more sophisticated loss function might allow the lens to modify larger parts of the image. A different loss function could successfully allow the lens to handle global shortcuts.

Further research is needed to evaluate the connection between *Shortcut Learning* and *Domain Generalization*: As pointed out by [26], shortcut learning might constitute a significant hurdle to domain generalization. Further, in some cases, it might be possible to assume that the simple features (i.e. shortcuts) constitute the majority of the expected distribution shift between source and target domain. In these cases, solving shortcut learning would also solve the domain generalization problem.

## 7 Conclusion

The ability to train a CNN classifier despite the known or unknown presence of shortcuts in the data is important. We present an architecture that can train on such data while still paying attention to the important features of the dataset. This is done by adding a lens network in front of the classifier we want to train. The lens is trained to detect and neutralize shortcuts by adversarial training on the classifier loss - removing features that the classifier pays attention to. The limited capacity of the network and an additional reproduc-

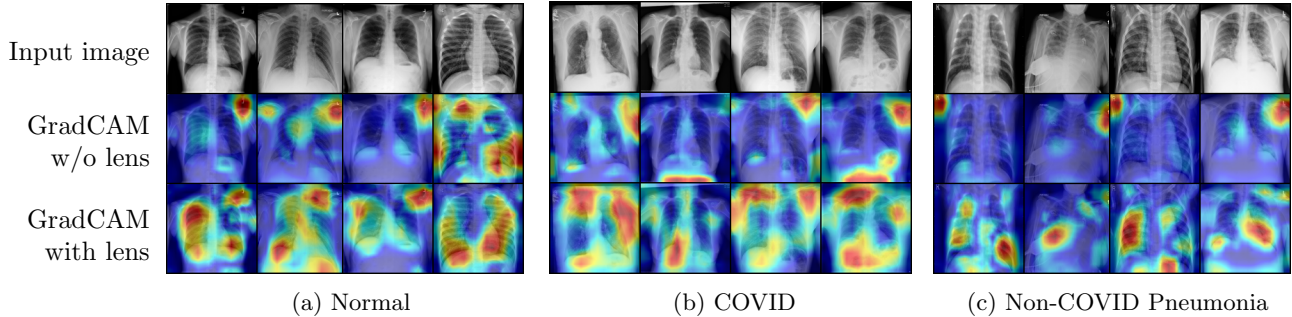


Figure 5: GradCAM images showing network attention when training on the covid-qu-Ex dataset. **Row 1** is the input image from the validation set. **Row 2** is the attention of a network trained without a lens. **Row 3** is the attention of a network trained with an attention lens.

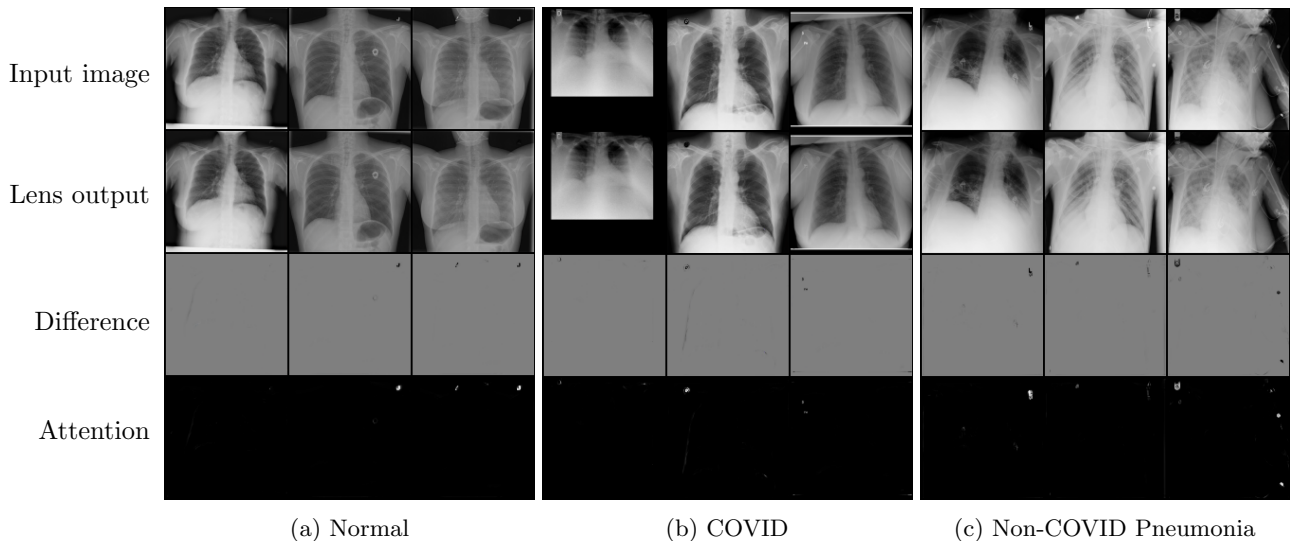


Figure 6: Example output of lens output and attention on x-ray images from the covid-qu-Ex dataset for the 3 classes COVID, Non-COVID Pneumonia, and Normal. **Row 1** shows original images. **Row 2** shows the output of the lens. **Row 3** shows the difference between rows 1 and 2. **Row 4** shows the output of the attention network  $A$ .

tion loss ensures the lens is only removing simple and semantically meaningless features (i.e. shortcuts).

We evaluate the performance of our architecture through commonly used datasets for image processing benchmarks, where we have added our own shortcuts. We find that the lens is able to ensure that the classifier pays attention to real features - often with similar quality as when trained on a dataset without any shortcuts. Finally, we show that the lens architecture can also handle a real-world dataset: a COVID chest x-ray dataset. We show that the lens is removing the text and symbols that are present on the x-ray images and that the classifier pays more attention to the desired lung area as a result.

## References

- [1] The pascal visual object classes challenge 2007 (voc2007). <http://host.robots.ox.ac.uk/pascal/VOC/voc2007/index.html>. (Accessed on 08/03/2022). 1, 2
- [2] Shumeet Baluja and Ian Fischer. Adversarial Transformation Networks: Learning to Generate Adversarial Examples. *arXiv:1703.09387 [cs]*, Mar. 2017. 2
- [3] Sara Beery, Grant Van Horn, and Pietro Perona. Recognition in terra incognita. In *Proceedings of the European Conference on Computer Vision (ECCV)*, 9 2018. 2
- [4] Nikolay Dagaev, Brett D. Roads, Xiaoliang Luo, Daniel N. Barry, Kaustubh R. Patil, and Bradley C. Love. A Too-Good-to-be-True Prior to Reduce Short-



- cut Reliance. *arXiv:2102.06406 [cs]*, Oct. 2021. arXiv: 2102.06406. **2**
- [5] Alex J DeGrave, Joseph D Janizek, and Su-In Lee. Ai for radiographic covid-19 detection selects shortcuts over signal. *Nature Machine Intelligence*, 3(7):610–619, 2021. **2, 4**
- [6] Carl Doersch, Abhinav Gupta, and Alexei A. Efros. Unsupervised visual representation learning by context prediction. In *Proceedings of the IEEE International Conference on Computer Vision (ICCV)*, 12 2015. **2**
- [7] Robert Geirhos, Jörn-Henrik Jacobsen, Claudio Michaelis, Richard Zemel, Wieland Brendel, Matthias Bethge, and Felix A. Wichmann. Shortcut Learning in Deep Neural Networks. *Nature Machine Intelligence*, 2(11):665–673, Nov. 2020. arXiv: 2004.07780. **2**
- [8] Spyros Gidaris, Praveer Singh, and Nikos Komodakis. Unsupervised Representation Learning by Predicting Image Rotations. *arXiv:1803.07728 [cs]*, Mar. 2018. arXiv: 1803.07728. **2**
- [9] Kaiming He, Xiangyu Zhang, Shaoqing Ren, and Jian Sun. Deep residual learning for image recognition. In *2016 IEEE Conference on Computer Vision and Pattern Recognition (CVPR)*, pages 770–778, 2016. **4**
- [10] Sergey Ioffe and Christian Szegedy. Batch normalization: Accelerating deep network training by reducing internal covariate shift. In *International conference on machine learning*, pages 448–456. PMLR, 2015. **3**
- [11] Alex Krizhevsky, Geoffrey Hinton, et al. Learning multiple layers of features from tiny images. 2009. **4**
- [12] Sebastian Lapuschkin, Stephan Wäldchen, Alexander Binder, Grégoire Montavon, Wojciech Samek, and Klaus-Robert Müller. Unmasking clever hans predictors and assessing what machines really learn. *Nature communications*, 10(1):1–8, 2019. **1, 2**
- [13] Ninareh Mehrabi, Fred Morstatter, Nripsuta Saxena, Kristina Lerman, and Aram Galstyan. A survey on bias and fairness in machine learning. *ACM Computing Surveys (CSUR)*, 54(6):1–35, 2021. **7**
- [14] Matthias Minderer, Olivier Bachem, Neil Houlsby, and Michael Tschannen. Automatic Shortcut Removal for Self-Supervised Representation Learning. pages 6927–6937. PMLR, Nov. 2020. **2, 3**
- [15] Nicolas M. Müller, Franziska Dieckmann, Pavel Czempin, Roman Canals, Konstantin Böttinger, and Jennifer Williams. Speech is Silver, Silence is Golden: What do ASVspoof-trained Models Really Learn? *arXiv:2106.12914 [cs, eess]*, Sept. 2021. **2**
- [16] Omid Poursaeed, Isay Katsman, Bicheng Gao, and Serge Belongie. Generative adversarial perturbations. In *Proceedings of the IEEE Conference on Computer Vision and Pattern Recognition (CVPR)*, June 2018. arXiv: 1712.02328 version: 3. **2**
- [17] Albert Pumarola, Antonio Agudo, Aleix M. Martinez, Alberto Sanfeliu, and Francesc Moreno-Noguer. GANimation: Anatomically-aware Facial Animation from a Single Image. **3**
- [18] Olaf Ronneberger, Philipp Fischer, and Thomas Brox. U-net: Convolutional networks for biomedical image segmentation. In *International Conference on Medical image computing and computer-assisted intervention*, pages 234–241. Springer, 2015. **2**
- [19] Olga Russakovsky, Jia Deng, Hao Su, Jonathan Krause, Sanjeev Satheesh, Sean Ma, Zhiheng Huang, Andrej Karpathy, Aditya Khosla, Michael Bernstein, Alexander C. Berg, and Li Fei-Fei. ImageNet Large Scale Visual Recognition Challenge. *International Journal of Computer Vision (IJCV)*, 115(3):211–252, 2015. **4**
- [20] Ramprasaath R. Selvaraju, Michael Cogswell, Abhishek Das, Ramakrishna Vedantam, Devi Parikh, and Dhruv Batra. Grad-cam: Visual explanations from deep networks via gradient-based localization. In *Proceedings of the IEEE International Conference on Computer Vision (ICCV)*, Oct. 2017. **6**
- [21] Anas M. Tahir, Muhammad E. H. Chowdhury, Amith Khandakar, Tawsifur Rahman, Yazan Qiblawey, Uzair Khurshid, Serkan Kiranyaz, Nabil Ibtehaz, M. Sohel Rahman, Somaya Al-Maadeed, Sakib Mahmud, Maymouna Ezeddin, Khaled Hameed, and Tahir Hamid. COVID-19 infection localization and severity grading from chest X-ray images. *Computers in Biology and Medicine*, 139:105002, Dec. 2021. **2, 4**
- [22] Xin Wang, Junichi Yamagishi, Massimiliano Todisco, Héctor Delgado, Andreas Nautsch, Nicholas Evans, Md Sahidullah, Ville Vestman, Tomi Kinnunen, Kong Aik Lee, et al. Asvspoof 2019: A large-scale public database of synthesized, converted and replayed speech. *Computer Speech & Language*, 64:101114, 2020. **2**
- [23] Chaowei Xiao, Bo Li, Jun-Yan Zhu, Warren He, Mingyan Liu, and Dawn Song. Generating Adversarial Examples with Adversarial Networks. *arXiv:1801.02610 [cs, stat]*, Feb. 2019. arXiv: 1801.02610. **2**
- [24] Bing Xu, Naiyan Wang, Tianqi Chen, and Mu Li. Empirical evaluation of rectified activations in convolutional network. *arXiv preprint arXiv:1505.00853*, 2015. **3**
- [25] John R. Zech, Marcus A. Badgeley, Manway Liu, Anthony B. Costa, Joseph J. Titano, and Eric Karl Oermann. Variable generalization performance of a deep learning model to detect pneumonia in chest radiographs: A cross-sectional study. *PLOS Medicine*, 15(11):e1002683, Nov. 2018. **2, 4**
- [26] Kaiyang Zhou, Ziwei Liu, Yu Qiao, Tao Xiang, and Chen Change Loy. Domain generalization: A survey. *IEEE Transactions on Pattern Analysis and Machine Intelligence*, pages 1–20, 2022. **1, 2, 7**